Available online at www.sciencedirect.com
SCIENCE DIRECT®
Journal of Molecular Catalysis A: Chemical 212 (2004) 211–217
JOURNAL OF MOLECULAR CATALYSIS A: CHEMICAL
www.elsevier.com/locate/molcata

Combination of CO_2 reforming and partial oxidation of methane over Ni/BaO-SiO_2 catalysts to produce low H_2/CO ratio syngas using a fluidized bed reactor

Qiangshan Jing [a,b], Hui Lou [a], Liuye Mo [a], Jinhua Fei [a], Xiaoming Zheng [a,*]

[a] *Institute of Catalysis, Zhejiang University, Hangzhou 310028, PR China*
[b] *Department of Chemistry, Xinyang Normal University, Xinyang 464000, PR China*

Received 1 August 2003; received in revised form 18 September 2003; accepted 26 October 2003

Abstract

The Ni/SiO_2 catalyst was modified by BaO in order to improve the thermal stability and the carbon deposition resistance during the combination of CO_2 reforming and partial oxidation of methane using a fluidized bed reactor, it is possible to convert methane into syngas with low H_2/CO ratio ($1 < H_2/CO < 2$) at above 85% methane conversion without catalyst deactivation in 10 h, in a most energy efficient and safe manner, requiring little or no external energy. Samples of the catalysts were characterized using TPR, X-ray diffraction (XRD) and TEM techniques, indicate that Ni agglomerating is a major reason for deactivation, addition of BaO might be responsible for its high activity and resistance to sintering because it can produce a highly dispersed active surface area as bound-state Ni species when the catalyst is prepared at high calcined temperatures. The addition of BaO as silica gel modifiers can be beneficial for the performance of the Ni/SiO_2 catalyst.

Keywords: Ni/BaO-SiO_2 catalyst; CO_2 reforming; Partial oxidation of CH_4; Fluidized bed reactor

1. Introduction

Synthesis gas is a versatile feedstock for the methanol and Fischer–Tropsch synthesis and several other carbonylation, hydrogenation and reduction reactions. In recent years, major research efforts have been concentrated on the CO_2 reforming [1–7] and the partial oxidation [8–12]. Like the steam reforming, the dry CO_2 reforming is also highly endothermic requiring a large energy input, while the partial oxidation is mildly exothermic with potential hazards due to the presence of hot spots.

Some researches studies about combining CO_2 reforming and partial oxidation of methane using a fixed bed reactor have been carried out [13–18], the product ratio of H_2/CO and thus the selectivity for various Fischer–Tropsch synthesis products can be controlled by changing the feed composition. In these cases, the exothermic combustion and the successive endothermic reforming caused significant temperature gradient in the catalyst bed [19]. The fluidized bed reactor is an attractive option in the syngas production due to the combination of combustion and reforming. This is because the fluidized bed reactor provides a high rate of heat transfer in order to maintain the isothermal operation [20] and also because the permanent circulation of the catalyst particles favors the burning of carbon on it the oxygen-rich zone of the catalyst bed [21], The use of the solid catalyst as a heat carrier can resolve the hot spot problem and fluidization has quite a favorable effect on the inhibition of carbon deposition [13]. In addition, the fluidization causes the re-reduction of oxidized catalyst and regenerates the active site for the methane reforming [22].

Our previous researches have shown the Ni/Al_2O_3 and Pt/$CoAl_2O_4$/Al_2O_3 catalysts provide high activity for the combined reaction using fluidized bed reactor [23,24]. In this study, we investigate the coupling between the exothermic partial oxidation methane and the endothermic CO_2 reforming of methane over the reduced Ni/BaO-SiO_2 catalysts in fluidized bed reactor, manipulating the reaction conditions (viz. temperature and relative concentration of CH_4, CO_2 and O_2 in the feed), one can control the H_2/CO ratio and

* Corresponding author. Tel.: +86-571-88273272; fax: +86-571-88273283.
E-mail address: zhengxm@zju.edu.cn (X. Zheng).

1381-1169/$ – see front matter © 2003 Elsevier B.V. All rights reserved.
doi:10.1016/j.molcata.2003.10.041

thus the selectivity for various Fischer–Tropsch synthesis products.

2. Experimental

2.1. Catalyst preparation

Modified supports were prepared by impregnating SiO_2 (supplied from Qingdao, Strem: $S_{BET} = 374\,m^2/g$, particle size: Ø = 0.28–0.45 mm) with an aqueous solution of barium nitrate. Followed by overnight drying at 383 K, the supports were subsequently calcined at 773 K in air for 4 h. The support nickel catalysts (metal loading, 5 wt.%) were prepared on $BaO–SiO_2$ by the wet impregnation method using $Ni(NO_3)_2{\cdot}6H_2O$ as the metal precursor, the catalyst was calcined in air at 973 K for 4 h before used . Ni and Ba loading means wt.% Ni or wt.% Ba in the catalyst and denoted as $Ni/BaO–SiO_2$.

2.2. Catalytic reaction

All the catalysts were tested under atmospheric pressure in a fluidized bed reactor, the reactor had its quartz tube (i.d. = 20 mm, H = 750 mm) inside a larger quartz furnace. A stainless steel net was used as a distributor in the fluidized bed reactor. A thermocouple that was connected to a PID temperature controller was placed out the quartz tube and in the middle of the catalyst bed. Pretreatment of catalysts was carried out by H_2 reduction at 923 K for 1 h under hydrogen flow at atmospheric pressure before the reaction. Feed gases with a C/O ratio of 1 were introduced into the reactor at a total flow rate of 18,000 cm^3/min for 2 cm^3 catalyst after reduction. An ice bath was set between the reactor exit and a sampling port for gas chromatograph analysis in order to remove water from the effluent gas. The gas compositions of reactants and products were analyzed with a GC (SHIMADZU-8A) equipped with a packed column (TDX-01) and a thermal conductivity detector.

2.3. Catalytic characterization

X-ray diffraction (XRD) data were obtained on a Rigaku-D/max-B automate power X-ray diffractometer. Anode Cu Kα(45 kV, 40 mA) was used as the X-ray source. The calcined catalysts were examined at a scanning rate of 2 min and the obtained X-ray diffraction patterns to identify the major phases present. Before TPR experiment, the catalyst was treated at 573 K for 30 min in Ar (99.999%) flow. After the sample was cooled down to 303 K, the temperature of the sample was increased from 323 to 973 K with the ramp of 20 K/min, 10%H_2/Ar mixture (30 cm^3/min) purging with the sample.

3. Results and discussion

3.1. Catalytic activity measurement

The combined reaction was carried out over the reduced $5Ni/BaO–SiO_2$ catalysts at 1023 K and the space velocity of 9000 h^{-1}. The time-dependent conversions of CH_4 are plotted in Fig. 1. Nickel species was regarded as the reactive site for this combined reaction and nickel loading was uniform on all the test samples, therefore, it is no evident effect on the initial activity for Ba loading, but there was great difference

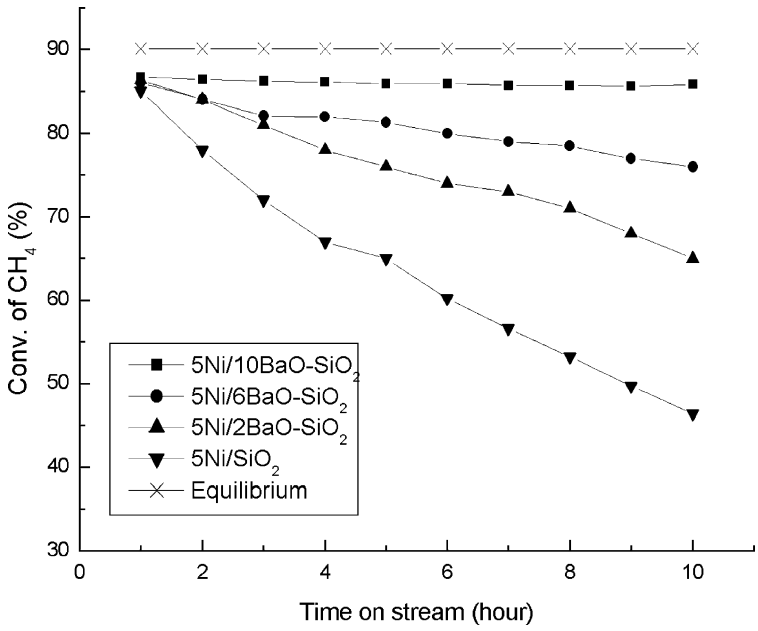

Fig. 1. Effect of Ba loading on the conversion of CH_4. Reaction conditions: T = 1023 K, CH_4:CO_2:O_2 = 1:0.4:0.3, GHSV = 9000 h^{-1}.

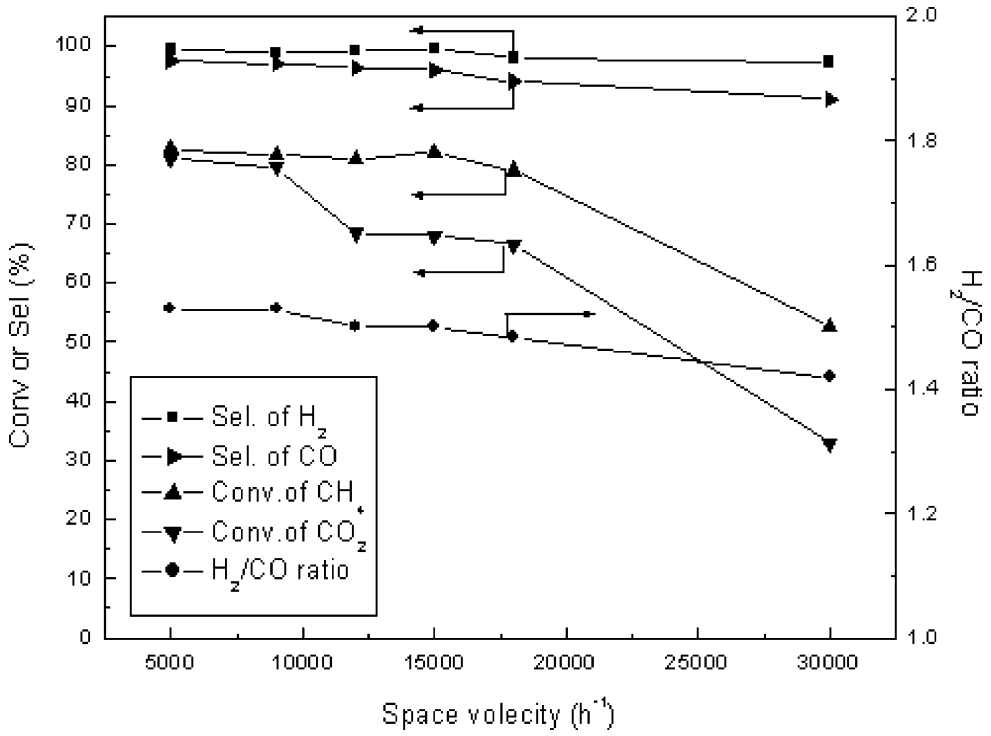

Fig. 2. CH_4 conversion, CO_2 conversion and H_2/CO ratio as a function of space velocity over the 5Ni/10BaO-SiO_2 catalyst (data obtained after 3 h reaction). $T = 1023$ K, CH_4:CO_2:O_2 = 1:0.4:0.3.

in the catalytic stability. However, when the Ba loading was below 8 wt.%, especially for Ba-free nickel-based catalyst, it was rapidly deactivated in 3 h on stream. The stability of 5Ni/BaO-SiO_2 was remarkably enhanced when the Ba loading above 8 wt.%. The catalytic activity of 5Ni/10BaO-SiO_2 did not decrease in 10 h on stream.

The space velocity was varied by changing the amount of catalyst while maintaining the total flow rate at 300 cm^3/min. The effect of space velocity on the steady-state activity of 5Ni/10BaO-SiO_2 and the product H_2/CO ratio is presented in Fig. 2. With increasing space velocity, the smaller was the gradient of CH_4 conversion decrease, the conversions of CH_4 and CO_2 decreased. In contrast, during the partial oxidation reaction, CH_4 conversion remained unchanged with increasing space velocity because of the presence of hot spots [17]. However, for the combined reaction, hot spots, less bright than in the partial oxidation of methane, have been observed visually. Consequently, the combined reaction can be operated in a more efficient manner than CO_2 reforming and in a safer manner than the partial oxidation. Fig. 2 also shows that, with increasing space velocity, the selectivity to H_2 is unchanged, while the selectivity to CO and the ratio H_2/CO decrease slightly.

Fig. 3 presents the influence of feed gas ratio on the catalytic activity of 5Ni/10BaO-SiO_2. The effect of the O_2/CO_2 ratio was investigated for a C/O ratio of 1 and a total flow rate of 300 cm^3/min. The CH_4 conversion increased with the ratio increasing of O_2/CO_2, but the CO_2 conversion passes through a maximum, at low O_2/CO_2 ratios, the conversion of CO_2 increases with increasing O_2 concentration. At high O_2/CO_2 ratios, the CO_2 concentration in the feed gas is low, but CO_2 is formed via the combustion of CH_4. The H_2 selectivity declined for some of H_2 being oxidized with increasing O_2 content in feed gas. The selectivity of CO was almost not changed. The H_2/CO ratios obtained in the CO_2 reforming of methane (in the absence of O_2) and in the partial oxidation of methane (in the absence of CO_2) were around 1.0 and 2.0, respectively. The combined partial oxidation and CO_2 reforming methane can provide a synthesis gas with a H_2/CO ratio between 1.0 and 2.0, which increases with increasing O_2/CO_2 ratio.

As showed in Fig. 4, when the reduction temperature was 823 K, mainly total oxidation of methane occurs. It is well known that Ni^{2+} is active for total oxidation of CH_4 but not for partial oxidation or CO_2 reforming of CH_4, while Ni^0 is the active component both for the partial oxidation of CH_4 and for the CO_2 reforming reaction [25,26]. The catalytic activity reach maximum until the reduction temperature is above 923 K. This result indicates that the active site is enough for this reaction at 923 K for reduction using the fluidized reactor.

The effect of reaction temperature on the steady-state activity of 5Ni/10BaO-SiO_2 is shown in Fig. 5, the conversion of CH_4 and CO_2 monotonically increased with increasing of reaction temperature, however, the selectivity of H_2 and CO increase slightly when the reaction temperature is above 973 K. Because reforming CH_4 with H_2O and CO_2 is an endothermic reaction and an increasing reaction temperature

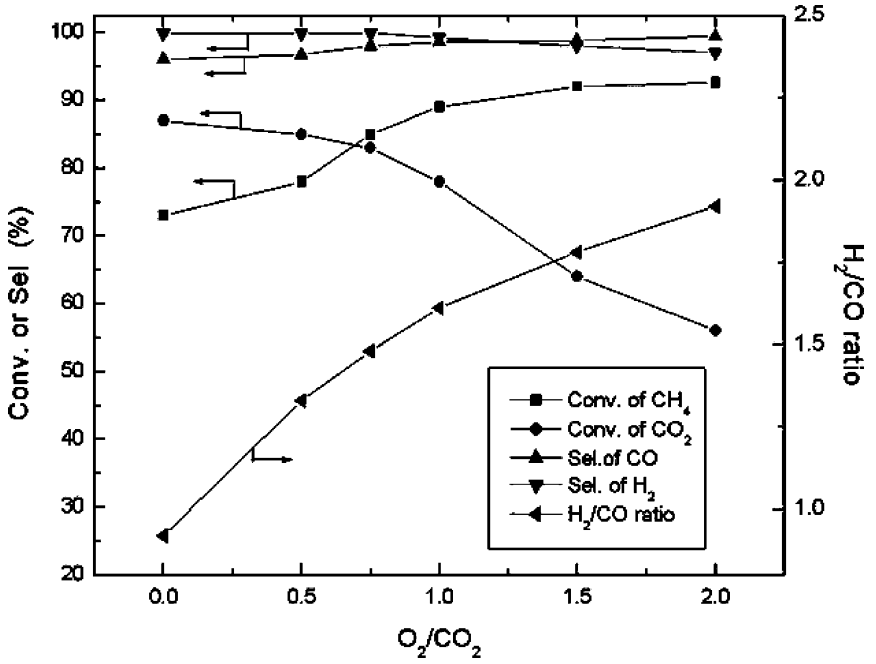

Fig. 3. Influence of O_2/CO_2 ratio in the feed on the conversion, selectivity and H_2/CO product ratio in the combining process at 1023 K (GHSV = 9000 h^{-1}).

shifts the reaction to production. It indicated that higher temperature was favor to produce H_2 and CO, and lower temperature would lead to combustion of CH_4.

3.2. Catalyst characterization

Fig. 6 gives XRD patterns of 5Ni/BaO-SiO_2 and 10BaO/SiO_2. The intensities of nickel peaks were influenced by addition of BaO, the higher was the BaO loading on catalyst, the weaker and broader become diffraction peaks due to Ni, this suggests that smaller nickel particles are formed in catalysts of higher BaO loading, no bulk nickel peaks appear in XRD pattern of 10BaO/SiO_2. Addition of Ba segregated the particle size of nickel, however, BaO itself as a support formed large nickel particles probably due to its small surface area, this indicates that the BaO is

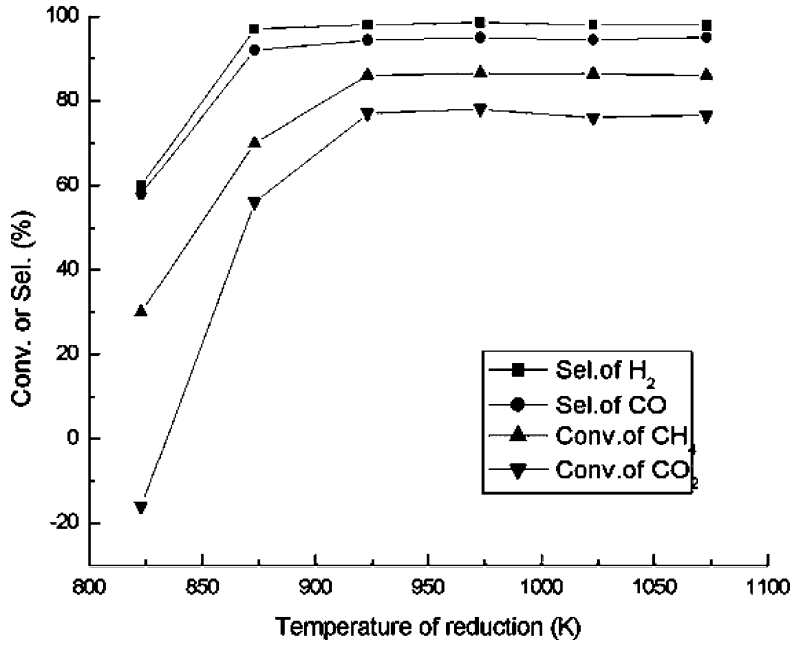

Fig. 4. Effect of the pretreated temperature on CH_4, CO_2 conversion and H_2, CO selectivity. Reaction conditions: reaction temperature 1023 K; feed gas ratio CH_4:CO_2:O_2 = 1:0.4:0.3; GHSV = 9000 h^{-1}.

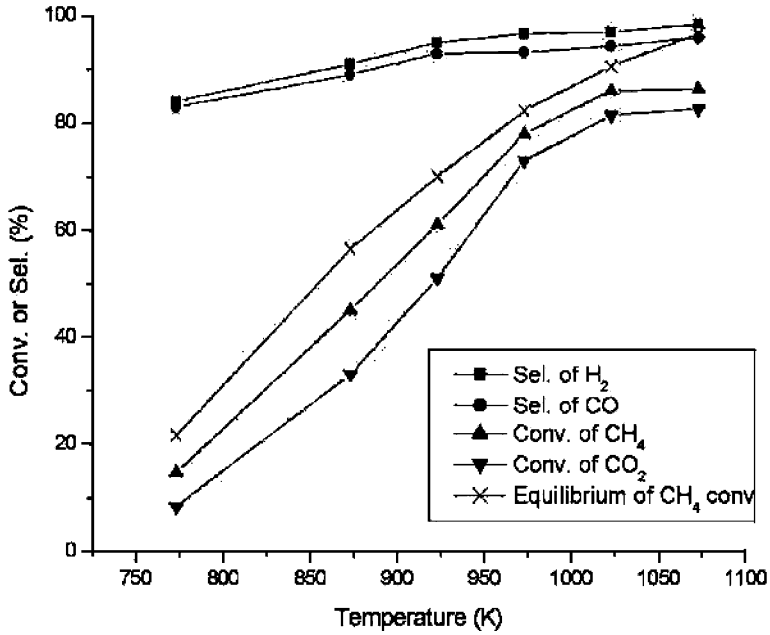

Fig. 5. Effect the reaction temperature on the 5Ni/10BaO-SiO_2 catalytic activity. Reaction conditions: CH_4:CO_2:O_2 = 1:0.4:0.3, GHSV = 9000 h^{-1}.

highly dispersed on the support of SiO_2 and it promotes the dispersion of NiO. The of NiO particle sizes, measured using XRD, are 46.1 and 82.9 nm of fresh and used catalyst, respectively. It can be showed that Ni aggregation dominated the activity change. Ni particles could be highly dispersed on BaO-modified SiO_2 support, which impeded the Ni particles aggregation during time on stream. The BaO-modified 5Ni/SiO_2 catalyst, therefore, has a higher stability. Accordingly, the highly dispersed Ni particles can be easily reduced, which leads to an initially much active catalyst.

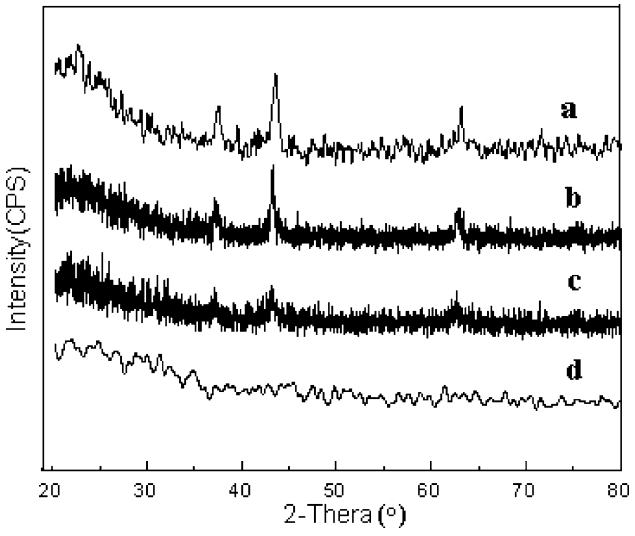

Fig. 6. XRD spectra of (a) 5Ni/SiO_2 (b) 5Ni/2BaO-SiO_2 (c) 5Ni/8BaO-SiO_2 (d) 5Ni/10BaO-SiO_2.

TEM micrograph of the 5Ni/SiO_2 and 5Ni/10BaO-SiO_2 catalysts (Fig. 7A and B, respectively) provided clear evidence of nickel oxide particles distribution on support. In the case of Ni/SiO_2 catalyst, nickel particles were not uniformly distributed on the surfaces, with a diameter ranging between 20 and 60 nm. However, nickel particles were segregated and dispersed in the 5Ni/10BaO-SiO_2 catalysts (Fig. 7B).

The reducibility of the Ni/BaO-SiO_2 catalysts was studied by TPR under 5%H_2/Ar flow in the range from 323 to 1073 K, presented in Fig. 8. Because a very weak interaction between Ni and SiO_2, the microcrystalline nickel oxide has been reported as the free state of the Ni active phase because of its mobility, which leads to migration, aggregation and growth of particles at high temperatures so that the dispersion of the active phase rapidly decreases, which is one of the main reasons why the supported Ni-based catalyst is easily deactivated. It can be seen that the predominant phase is that which a strong interaction between Ni and BaO-modified SiO_2. This interaction become stronger with increasing barium loading. This shifting of the reduction profile to higher temperatures is due to the strong metal support interactions and to the presence of calcium as it has been reported in the literature [27,28]. When prepared by wet impregnation on BaO-modified support at high calcined temperatures, the nickel ions tend to be highly dispersed and can be segregated. Although reduction is difficult, at least above 893 K, it exhibits very activity and resistant to sintering once reduced, these bound state Ni particles remain highly dispersed due to their very low mobility, so they have long life and good stability. XRD results were also in agreement with TPR results, signals related to BaO or to interaction

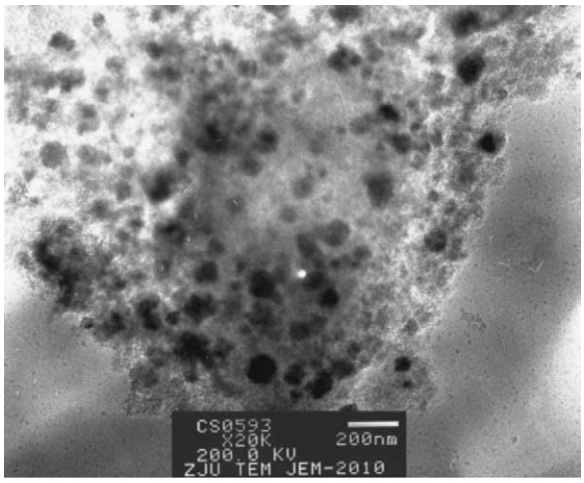

(A)

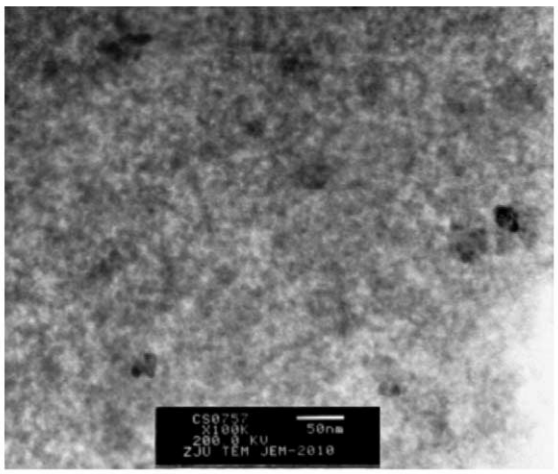

(B)

Fig. 7. (A) TEM photography of 5Ni/SiO_2 catalyst. (B) TEM photography of 5Ni/10BaO-SiO_2 catalyst.

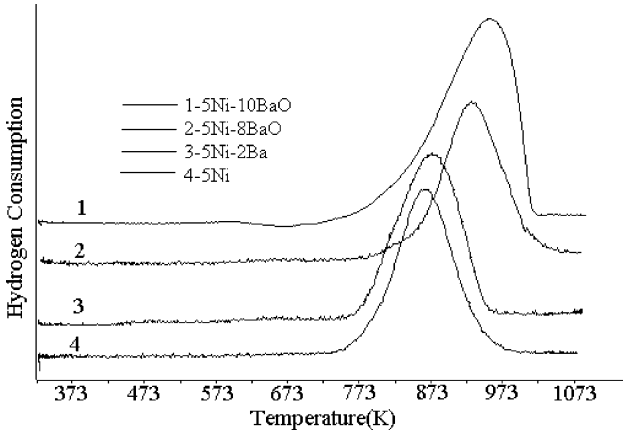

Fig. 8. H_2-TPR profiles of 5%Ni/BaO-SiO_2 catalysts.

compounds between the modifier and the support were not detected.

4. Conclusion

By combining the endothermic and exothermic reactions of methane with CO_2 and O_2 over BaO-SiO_2 catalyst using fluidized bed reactor, methane can be converted to syngas with low H_2/CO ratio required for Fischer–Tropsch synthesis, by changing the O_2/CO_2 ratio of the feed gases, the ratio of the products H_2/CO can be controlled between 1 and 2. The nickel particles tend to be highly dispersed and can be fixed by being segregated in BaO-modified support, which had a significant effect on its reduction behavior and show good resistance to aggregation of the nickel particles. These catalysts present high stability and activity with respect to the Ni/SiO_2. This combining reaction can be run in a most energy efficient and safe manner in a fluidized bed reactor.

Acknowledgements

This research project is supported by Natural Science Foundation of Zhejiang province.

References

[1] A.H.J. van Keulen, K. Seshan, J.H.B.J. Hoebink, J.R.H. Ross, J. Catal. 166 (1997) 306.
[2] C.J. Huang, X.M. Zheng, L.Y. Mo, J.H. Fei, Chin. J. Chem. 4 (2001) 340.
[3] A.N.J. van Keulen, M.E.S. Hegarty, J.R.H. Ross, P.F. van den Oosterkamp, Stud. Surf. Sci. Catal. 107 (1997) 537.
[4] C.J. Huang, J.H. Fei, D.J. Wang, X.M. Zheng, Chin. Chem. Lett. 2 (2000) 181.
[5] C.J. Huang, X.M. Zheng, L.Y. Mo, J.H. Fei, Chin. Chem. Lett. 3 (2001) 249.
[6] A.A. Lemonidou, I.A. Vasalos, Appl. Catal. A. 228 (2002) 227.
[7] J.R.H. Ross, A.N.J. van Keulen, M.E.S. Hegarty, K. Seshan, Catal. Today 30 (1996) 193.
[8] E. Ruckenstein, H.Y. Wang, J. Catal. 187 (1999) 151.
[9] F. Basile, G. Fornasari, F. Trifiro, A. Vaccari, Catal. Today 64 (2001) 21.
[10] E. Ruckenstein, Y.H. Hu, Appl. Catal. A. 183 (1999) 85.
[11] K. Opoku-Gyamfi, A.A. Adesina, Appl. Catal. A. 180 (1999) 113.
[12] D.A. Hickman, L.D. Schmidt, Science 259 (1993) 343.
[13] A.L. Larents, N.S. de Resende, V.M.M. Salim, J.C. Pinto, Appl Catal A: Gen. 215 (2001) 211.
[14] A.M. Oonnor, J.R.H. Ross, Catal. Today 46 (1998) 203.
[15] K. Tomishige, Y. Matsuo, Y. Yoshinaga, Y. Sekine, M. Asadullah, K. Fujimoto, Appl. Catal A: Gen. 223 (2002) 225.
[16] K. Tomishige, S. Kanazawa, K. Suzuki, M. Asadullah, M. Sato, K. Ikushima, K. Kunimori, Appl. Catal A: Gen. 233 (2002) 35.
[17] E. Ruckstein, H.H. Hu, Ind. Eng. Chem. Res. 37 (1998) 1744.
[18] E. Ruckstein, H.Y. Wang, Catal. Lett. 73 (2001) 99.
[19] A.M. De Groote, G.F. Froment, Appl. Catal. A. 138 (1996) 245.
[20] U. Olsbye, E. Tangstad, I.M. Dahl, Stud. Surf. Sci. Catal. 81 (1994) 303.
[21] A. Santos, M. Menendez, A. Monzon, J. Santamaria, E.E. Miro, E.A. Lombardo, J. Catal. 158 (1996) 83.

[22] Y. Matsuo, Y. Yoshinaga, Y. Sekine, K. Tomishige, K. Fujimoto, Catal. Today 63 (2000) 439.
[23] L. Mo, J. Fei, C. Huang, X. Zheng, J. Mol. Catal A: Chem. 93 (2003) 177.
[24] L. Mo, X. Zheng, Y. Chen, J. Fei, React. Kinet. Catal. Lett. 78 (2003) 237.
[25] F. Fischer, H. Tropsch, Brennst Chem. 9 (1928) 29.
[26] I.M. Brdov, L.O. Apel Baum, Kinet. Katal. 5 (1964) 696.
[27] J.T. Richardon, B. Turk, M.V. Twigg, Appl. Catal. A. 97 (1996) 148.
[28] Zheng Xu, Yumin Li, Jiyan Zhang, Liuchang, Rongqi Zhou, Zhangting Duan, Appl. Catal A. 210 (2001) 45.